Vascular Pharmacology 115 (2019) 46–54

Contents lists available at ScienceDirect

Vascular Pharmacology

journal homepage: www.elsevier.com/locate/vph

Lipid core nanoparticles as vehicle for docetaxel reduces atherosclerotic lesion, inflammation, cell death and proliferation in an atherosclerosis rabbit model

Bianca C. Meneghini[a], Elaine R. Tavares[a], Maria C. Guido[a], Thauany M. Tavoni[a], Helio A. Stefani[b], Roberto Kalil-Filho[a], Raul C. Maranhão[a,b,*]

[a] Heart Institute (InCor), Medical School Hospital, University of São Paulo, São Paulo, Brazil
[b] Faculty of Pharmaceutical Sciences, University of São Paulo, São Paulo, Brazil

ARTICLE INFO

Keywords:
Lipid core nanoparticles
Docetaxel
Atherosclerosis
Inflammation
Drug delivery

ABSTRACT

Chemotherapeutic agents used in cancer treatment associated to nanoparticles (LDE) that mimic the composition of low-density lipoprotein and buffer their toxicity can have strong anti-atherosclerosis action, as we showed in cholesterol-fed rabbits. Here, a novel preparation of docetaxel (DTX) carried in LDE was evaluated. Eighteen rabbits were fed 1% cholesterol during 8 weeks. After the first 4 weeks, 9 animals were treated for 4 weeks with intravenous LDE-DTX (1 mg/kg/week) and 9 with LDE only (controls) once a week for 4 weeks. Animals were then euthanized and the aortas were analyzed for morphometry, immunohistochemistry and Western blot. LDE-DTX treated group showed 80% reduction of atheroma area compared to controls. LDE-DTX treatment reduced in 60% the protein expression of macrophage marker CD68 and of MCP-1 in 80%. LDE-DTX pronouncedly lowered expression of pro-inflammatory markers NF-κB, TNF-α, IL-1β, IL-6 and von Willebrand factor and elicited 40% reduction in cell proliferation marker PCNA. The presence of smooth muscle cells in the intima was 85% smaller than in controls. Pro-apoptotic caspase 3, caspase 9, Bax, and anti-apoptotic Bcl-2 all were reduced by LDE-DTX. Protein expression of MMP-2 and MMP-9, TGF-β, and collagen 1 and 3 were also markedly lowered by the LDE-DTX treatment. Animals showed no hematological, hepatic or renal toxicity consequent to LDE-DTX treatment. In conclusion, LDE-DTX showed a wide array of strong effects on pro-inflammatory and proliferation-promoting factors that drive the lesion development. These findings and the lack of observable toxicity indicate that LDE-DTX can be a candidate for future clinical trials.

1. Introduction

The development of atherosclerotic lesions is driven by a chronic inflammatory and proliferative process, with secretion of cytokines and other pro-inflammatory factors by the injured endothelium and inflammatory cells [1]. The proliferation of vascular smooth muscle cells (VSMCs) in the media layer, stimulated by growth factors from different sources and subsequent migration of VSMCs to the intima is also a key event in lesion development [2,3]. Recently the validity of anti-inflammatory strategies to prevent the manifestations of atherosclerosis was shown in the CANTOS study, in which the blockade of IL-1βby canakinumab achieved reduction of major adverse cardiovascular events [4].

Anti-cancer drugs are the most powerful anti-proliferative agents in the Pharmacopea, and possess notorious suppressor actions on the immune system: neutropenia and lymphopenia are the major side effects of those drugs [5]. In 2008, Maranhão et al. [6] proposed the use of those drugs to treat atherosclerotic lesions. Those authors had previously shown that association of chemotherapeutic agents to nanoparticles (LDE) similar to the lipid composition of low-density lipoprotein (LDL), but made without protein, pronouncedly reduced the toxicity of those agents, paving the way for their use in diseases other than cancer [7–9]. The treatment of rabbits with atherosclerosis induced by cholesterol feeding with paclitaxel carried in LDE resulted in marked reduction of the width and extension of the lesions. The macrophage invasion and VSMC presence in the intima were inhibited [6]. In subsequent studies also performed in cholesterol-fed rabbits, preparations of other anti-neoplastic drugs carried in LDE, such as LDE-

* Corresponding author at: Laboratório de Metabolismo e Lípides, Instituto do Coração (InCor) do Hospital das Clínicas da Faculdade de Medicina da Universidade de São Paulo (HCFMUSP), Av. Dr. Enéas de Carvalho Aguiar, 44, bloco 2, 1° subsolo, São Paulo – SP, Brazil.
E-mail address: ramarans@usp.br (R.C. Maranhão).

https://doi.org/10.1016/j.vph.2019.02.003
Received 20 December 2018; Received in revised form 17 January 2019; Accepted 19 February 2019
Available online 20 February 2019
1537-1891/

etoposide, LDE-methotrexate and LDE-carmustine have also shown, intense anti-atherosclerotic effects, similarly to LDE-paclitaxel [10–12]. The effect of LDE-paclitaxel of promoting atherosclerosis regression in the cholesterol-fed rabbits was increased by combining with the treatment with LDE-methotrexate [13].

Taxanes, such as paclitaxel and docetaxel (DTX), constitute an important class of cytotoxic agents. Taxanes inhibit the disassembly of microtubules and promoting microtubule polymerization [14]. Association of paclitaxel to LDE for injection into the bloodstream strongly diminished the clinical and laboratorial toxicity of this drug, as demonstrated in experimental animals and in studies with patients with advanced cancers [6,15–17]. The viability and safety of treatment with the LDE-paclitaxel formulation was also demonstrated in a pilot study enrolling patients with aortic atheromas [18]. The current study was aimed not only to investigate the action of docetaxel, the other major taxane, as carried in LDE on the extension of atherosclerotic lesions, intima width or cellularity but also the effects of this preparation on local pro-inflammatory and proliferation factors, apoptosis and collagen deposition that could be involved in the pro-atherogenesis mechanisms. The results showed not only that LDE-DTX has a potent anti-atherosclerosis action but also shed light on the action of DTX on non-neoplastic inflamed tissues.

2. Methods

2.1. Experimental protocol

Male New Zealand white rabbits from FMUSP (São Paulo, SP) weighing approximately 3.6 kg were housed in individual cages in a temperature-controlled room (20–22 °C), on a 12 h light/dark cycle during the experimental period and water was provided *ad libitum*. Animals were weighed weekly. For the atherosclerosis induction, animals were fed with 150 g/day of usual commercial diet increased with 1% cholesterol (weight/weight) during all experimental period of 8 weeks. The remaining portion of food was weighed daily to evaluate the amount of food intake during the study. The treatment began after the first 4 weeks of atherosclerosis induction. The animals were allocated to two experimental groups:

- Control group (n = 9): animals received intravenous administration of LDE alone once a week for 4 weeks;
- LDE-DTX group (n = 9): animal were treated with intravenous administration of the association LDE-DTX, at a dose of 1 mg/kg once a week for 4 weeks.

After the end of the experimental protocol, the animals were euthanized and the aortas were excised for morphometric, immunohistochemistry and protein expression analysis.

This study was approved by the Ethics Committee of the University of São Paulo.

2.2. Biochemistry and blood cell count

Blood samples of the rabbits were collected from the marginal ear vein before the beginning of the cholesterol-rich diet (baseline), before the beginning of the treatment with LDE-DTX or LDE alone (pre-treatment) and at the end of the study (post-treatment) for determination of total and high-density lipoprotein cholesterol (HDL-c), triglycerides, alanine aminotransferase (ALT), aspartate aminotransferase (AST), urea, creatinine, and for blood cell count. The analyses were performed using a COBAS c111 (Roche, Basel, Switzerland) and a veterinary hematology analyzer Poch 100iV Diff Sysmex-Roche (Roche, Batsel, Switzerland) at the Special Analysis Laboratory (LAR) of the Hospital das Clínicas, FMUSP.

2.3. Derivatization of docetaxel and preparation of LDE-DTX

To improve the association rate of DTX to LDE, the drug was derivatized to enhance the lipophilicity. DTX was diluted in anhydrous dichloromethane; to this was added oleic acid, DCC and DMAP. The mixture was stirred under an inert atmosphere for 2 h at room temperature. The reaction was monitored by high-performance liquid chromatography (HPLC), on silica C18 column (Agilent Technologies, Santa Clara, CA, USA), mobile phase methanol:acetonitrile (90,10 v/v), at 230 nm.

LDE was prepared from a lipid mixture consisting of 64% phosphatidylcholine, 33% esterified cholesterol, 1% non-esterified cholesterol and 2% triglycerides [18]. The aqueous phase consisting of 100 mg of polysorbate 80 (Tween 80, Merck, Hohenbrum, Germany) and 10 mL of Tris-HCl buffer pH 8.05 was kept at room temperature. The pre-emulsion was obtained by adding the hydrophilic phase to the oil phase by ultrasonic radiation until complete solubilization. Emulsification of all lipids and the aqueous phase was obtained by high-pressure homogenization using an Emulsiflex C5 homogenizer (Avestin Inc., Ottawa, Canada) for 30–40 min. To prepare LDE-DTX, DTX was added to the lipid mixture at a drug:lipid ratio of 1:10 and the nanoparticle was centrifuged at 1800 × *g* for 15 min to separate the unbound DTX that precipitates upon centrifugation. The particle size of both preparations was 60 nm, as measured by dynamic light scattering method at a 90° angle, using the ZetaSizer Nano ZS90 equipment (Malvern Instruments, Malvern, UK). The efficiency of the association of DTX to LDE was measured by HPLC. The nanoparticles were sterilized by passing through a 0.22 μm pore polycarbonate filter (EMD Millipore Corporation, Billerica, MA, USA) and kept at 4 °C until it was used.

2.4. Planimetry of atherosclerotic lesions

The aorta was excised from the aortic arch to the abdominal aorta, opened longitudinally and placed in 10% buffered formalin. After fixation, the lipid deposits in the aortas were stained by Scarlat R (Sudan IV; Sigma, Saint Louis, USA), and aortas were photographed to perform the measurements. Total area and lesion area of the aortas were measured using Image J image analysis software (National Institutes of Health, Bethesda, MA, USA) and the percentage of macroscopic atherosclerotic lesions was calculated by the ratio lesion area/total area × 100.

2.5. Morphometric analysis of the aortic arch

After the macroscopic analysis, the aortic arch of aortas were sectioned in 5 mm segments, embedded in paraffin and the 5 μm sections were stained in hematoxylin-eosin and Masson's trichrome. Intima layer area were measured using Leica QWin Image Analysis software under 100× magnification (Leica Q500 iW; Leica Imaging Systems, Cambridge, UK).

2.6. Immunohistochemistry

Additional sections of aortic arch were labeled for macrophages, VSMCs and a cell proliferation marker, PCNA (proliferating cell nuclear antigen). For immunostaining, antigen retrieval was performed with a Pascal antigen retrieval high-pressure chamber (Dako, Carpinteria, CA, USA) with 10 mM citrate buffer, pH 6.0 (macrophages) or 10 mM Tris-HCl, 1 mM EDTA, pH 9.0 (VSMCs and PCNA). Endogenous peroxidase activity was blocked by incubation in 3% hydrogen peroxide. The nonspecific reaction was blocked with 1% bovine albumin (Sigma-Aldrich, Burlington, MA, USA) for 1 h at 37 °C. The sections were then incubated overnight at 4 °C with the primary antibodies (Table 1). Next, the sections were incubated for 30 min at room temperature with SuperPicture Polymer Detection System (Invitrogen, Carlsbad, CA, USA).

Table 1
Primary antibodies used in this study.

Primary antibody name	Supplier	Catalog number	Dilution	Application
Anti-alpha actin	Dako	M0851	1:400	Immunohistochemistry
Anti-BAX	Abcam	Ab7977	1:500	Western blot
Anti-Bcl-2	Abcam	Ab59348	1:1000	Western blot
Anti-capase 3	Abcam	Ab2302	1:1000	Western blot
Anti-capase 9	Abcam	Ab32539	1:1000	Western blot
Anti-CD68	Abcam	Ab125212	1:1000	Western blot
Anti-collagen I	Abcam	Ab90395	1:1000	Western blot
Anti-collagen III	Abcam	Ab7778	1:1000	Western blot
Anti-GAPDH	Calbiochem	BC1001	1:10,000	Western blot
Anti-IL-1-beta	Abcam	Ab82558	1:1000	Western blot
Anti-IL-6	Abcam	Ab83339	1:1000	Western blot
Anti-MCP-1	Abcam	Ab25124	1:1000	Western blot
Anti-MMP-2	Abcam	Ab37150	1:1000	Western blot
Anti-MMP-9	Abcam	Ab137867	1:1000	Western blot
Anti-NF-κB	Abcam	Ab16502	1:1000	Western blot
Anti-PCNA	Abcam	Ab29	1:1000	Western blot
			1:100	Immunohistochemistry
Anti-RAM11	Dako	M0633	1:500	Immunohistochemistry
Anti-TNF-alpha	Abcam	Ab1793	1:1000	Western blot
Anti-von Willebrand	Abcam	Ab6994	1:1000	Western blot

The sections were then incubated with a 3.3′-diamino-benzidine (DAB) chromogen system (Dako, Carpinteria, CA, USA) for 2 min at room temperature and counterstained with hematoxylin. The colour detection threshold was chosen for the DAB chromogen in tissue sections. The image analysis of immunostaining for VSMCs was calculated by the percentage of the labeled area relative to the total intima layer area. The measurements were performed using the QWin Image Analysis software (Leica Imaging Systems, Cambridge, UK)under 100× magnification.

2.7. Western blot analysis

Fragments of 1 mg of aortic arch tissue were homogenized in 1 mL of RIPA lysis buffer (tris base pH 8.0, NaCl, NP-40, and glycerol) with the protein inhibitors: aprotinin, leupeptin and fluoromethylphenylsulfonyl. The proteins were size-fractionated on polyacrylamide/sodium dodecyl sulfate (SDS) gel; the separated proteins were then electrophoretically transferred to a nitrocellulose membrane. The membranes were blocked with 5% non-fat milk. After the primary antibodies (Table 1) were incubated overnight, the blots were washed and incubated with horseradish peroxidase-conjugated secondary antibodies (Calbiochem, San Diego, CA, USA). Bands were visualized using enhanced chemiluminescence (Amersham; GE, Fairfield, CT, USA), and exposed and analyzed using an image analyzer (Amersham Imager 600; GE, Fairfield, CT, USA). Values were normalized for expression of glyceraldehyde 3-phosphate dehydrogenase (GAPDH), and results were expressed as a percentage of Control group mean.

2.8. Statistical analysis

Data are expressed as mean ± standard error of the mean (SEM). The distribution of variables and the hypothesis of equality of variances were tested in all cases. For food intake, weight profile and laboratory analysis data, for normal distribution variables, we used the ANOVA test with Bonferroni post-test, to perform multiple comparisons. For non-normal distribution variables, we used the Kruskal-Wallis test with Dunn post-test. The *t*-Student test was used to analyze planimetry, morphometry, immunohistochemistry and Western blot assays. In all analyses, $p < .05$ was considered statistically significant. Statistical analyses were carried out using GraphPad Prism v.5 statistical software (GraphPad Software, Inc., La Jolla, CA).

3. Results

3.1. Body weight, food intake, biochemistry and blood cell count

The evolution of body weight (Fig. 1A) and food intake (Fig. 1B) was similar in the Control and in the LDE-DTX group during all experimental period.

Table 2 shows the lipid profile of Control and LDE-DTX groups at baseline, pre-and post-treatment. After 8 weeks of cholesterol rich diet, total cholesterol raised roughly 35-fold and HDL-c about 15-fold in both groups. Triglycerides also increased about 3-fold in both groups. There was no difference in urea, creatinine, ALT and AST in both groups (Table 2).

Regarding the hematological profile (Table 3), red blood cells decreased in both groups at the end of the protocol. Total leukocyte increased in both Control and LDE-DTX groups as well as the monocyte percentage. The platelet count that was similar in both groups of animals.

3.2. Atherosclerotic plaques analysis

LDE-DTX treated rabbits showed 80% less atherosclerotic area in aorta when compared to the control animals that received only LDE, as shown in Fig. 2A. Representative images of atherosclerotic plaques are depicted in Fig. 2B, stained in red [19]. Likewise, as shown in Fig. 2C and D, the microscopic lesion area was 85% lower in LDE-DTX animals compared with Control animals. The presence of VSMCs in intima layer was also 85% lower in LDE-DTX compared with Controls as shown in

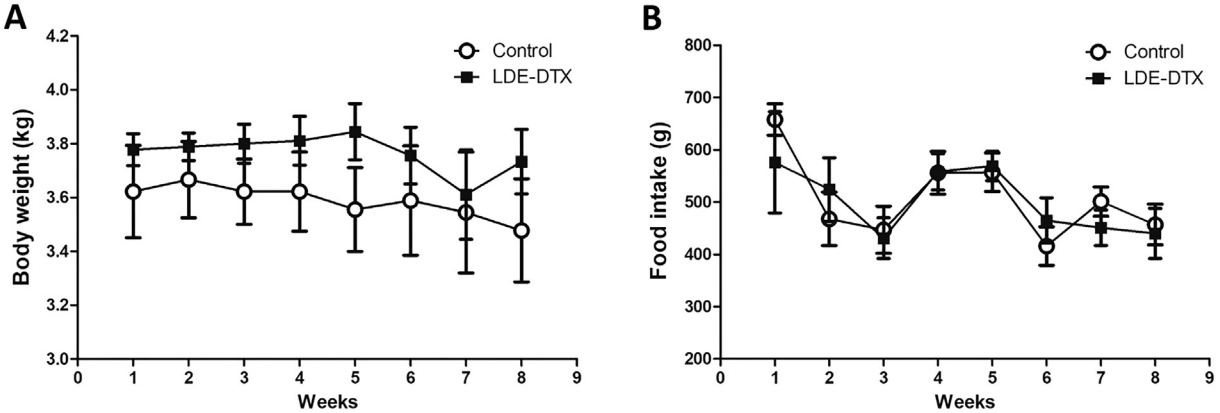

Fig. 1. Body weight and food intake. (A) Body weight (kg) of Control (n = 9) and LDE-DTX (n = 9) groups. (B) Food intake (g) of Control (n = 9) and LDE-DTX (n = 9) groups. Data are expressed as mean ± SEM in all plots. DTX, docetaxel.

Table 2
Biochemical analysis of rabbits from Control group (n = 9) and treated with LDE-DTX (n = 9) analyzed before the beginning of the cholesterol-rich diet (baseline), before the beginning of the treatment with LDE-DTX (pre-treatment) and at the end of the study (post-treatment).

	Control			LDE-DTX		
	Baseline	Pre-treatment	Post-treatment	Baseline	Pre-treatment	Post-treatment
Cholesterol (mg/dL)						
Total cholesterol	43 ± 3	1116 ± 53*	1850 ± 208‡,§	37 ± 3$^{\#}$	1036 ± 53$^{†,\|\|}$	1826 ± 408‡,**
HDL-c	23 ± 2	281 ± 23*	390 ± 87‡	20 ± 3$^{§,\#}$	239 ± 24$^{†,\|\|}$	284 ± 48$^{*,\$}$
Non-HDL-c	20 ± 2	849 ± 70†	1533 ± 166‡	17 ± 2$^{ø,\#}$	797 ± 46$^{†,\|\|}$	1542 ± 373‡,**
Triglycerides	65 ± 8	138 ± 31	207 ± 35*	69 ± 9$^{\&}$	129 ± 21	209 ± 32$^{*,\$}$
Urea (mg/dL)	30 ± 4	45 ± 4	49 ± 4	34 ± 3	53 ± 3	53 ± 4
Creatinine (mg/dL)	0.97 ± 0.03	1.46 ± 0.12	1.49 ± 0.21	0.96 ± 0.30	1.62 ± 0.10	1.71 ± 0.20
ALT (UI/L)	63 ± 10	71 ± 14	64 ± 9	74 ± 16	100 ± 31	63 ± 11
AST (UI/L)	32 ± 4	51 ± 13	61 ± 10	43 ± 8	57 ± 12	48 ± 6

Data are expressed as means ± SEM. HDL-c: high-density lipoprotein cholesterol; ALT: alanine aminotransferase; AST: aspartate aminotransferase.
* $p < .01$ *vs* Control baseline.
‡ $p < .001$ *vs* Control baseline.
§ $p < .01$ *vs* Control pre-treatment.
$^{\#}$ $p < .001$ *vs* Control post-treatment.
† $p < .05$ *vs* Control baseline.
$^{||}$ $p < .05$ *vs* LDE-DTX baseline.
** $p < .001$ *vs* LDE-DTX baseline.
$^{\$}$ $p < .01$ *vs* LDE-DTX baseline.
^{ø} $p < .05$ *vs* Control pre-treatment.
$^{\&}$ $p < .01$ *vs* Control post-treatment.

Fig. 2E and F.

3.3. Inflammation analysis

Fig. 3A shows representative Western blot bands of inflammatory markers in the aortic arch of LDE-DTX and Control groups. Protein expression of the macrophage marker CD68 was reduced in roughly 60% as shown in Fig. 3B. The diminished presence of macrophages in the atherosclerotic lesions of LDE-DTX group is shown in Fig. 3C. Similarly, the chemokine MCP-1 (monocyte chemoattractant protein-1) was also diminished by 80% in LDE-DTX group compared to Control group in the aortic arch (Fig. 3D).

The animals treated with LDE-DTX showed less protein expression of all inflammatory markers analyzed. LDE-DTX group protein expression of NF-κB (nuclear factor κ B), TNF-α, IL-1β and IL-6 was about 60% lower than Control group (Fig. 3E–H).

LDE-DTX treated group showed about 50% less protein expression of vWF (von Willebrand factor) than Control animals (Fig. 3I).

3.4. Cell proliferation and apoptosis analysis

Protein expression of the proliferation marker PCNA was 40% lower in the LDE-DTX treated group compared to the Control group (Fig. 4A–B). The illustrative image of PCNA presence in the aortic arch of Control and LDE-DTX groups is shown in Fig. 4C.

The representative Western blot bands of cell death markers in the aortic arch of Control and LDE-DTX groups are shown in Fig. 5A.The protein expression of pro-apoptotic proteins caspase 3 (Fig. 5B), caspase 9 (Fig. 5C) and Bax (Fig. 5D) were roughly 50% lower in LDE-DTX group compared to the Control group. The anti-apoptotic factor Bcl-2 protein expression was also 50% lower in LDE-DTX treated animals when compared to Control animals (Fig. 5E).

3.5. Vascular repair analysis

Fig. 6A shows representative Western blot bands of metalloproteinases (MMP) 2 and 9, TGF-β (transforming growth factor β), and collagens 1 and 3 of LDE-DTX and Control groups. The expression of MMP-

Table 3
Hematological profile of rabbits of Control group (n = 9) and LDE-DTX group (n = 9) analyzed before the beginning of the cholesterol-rich diet (baseline), before the beginning of the treatment with LDE-DTX (pre-treatment) and at the end of the study (post-treatment).

	Control			LDE-DTX		
	Baseline	Pre-treatment	Post-treatment	Baseline	Pre-treatment	Post-treatment
Erythrocytes (10^9/mL)	5.9 ± 0.4	4.3 ± 0.2*	3.8 ± 0.2**	6.7 ± 0.3‡,§	4.7 ± 0.2$^{\|\|}$	3.9 ± 0.2$^{**,\|\|}$
Leucocytes (10^6/mL)	11.5 ± 1.1	16.9 ± 1.3	22.5 ± 1.9**	12.1 ± 1.2§	17.5 ± 1.7	18.3 ± 1.4$^{\#}$
Lymphocytes (%)	53 ± 2.5	56 ± 0,1	61 ± 4.0	54 ± 2.9	55 ± 3.4	58 ± 2.6
Monocytes (%)	1.9 ± 0.5	2.6 ± 0.6	6.8 ± 1.1*,†	4.6 ± 0.6	6.9 ± 1.3*,†	6.2 ± 0.7‡
Neutrophils (%)	41.4 ± 3.4	38.2 ± 1.2	31.4 ± 3.4	41 ± 4.8	32.7 ± 2.4	34.9 ± 2.5
Platelets (10^3/mL)	231 ± 24	252 ± 41	318 ± 72	253 ± 29	262 ± 28	224 ± 18

Data are expressed as mean ± SEM.
* $p < .01$ *vs* Control baseline.
** $p < .001$ *vs* Control baseline.
‡ $p < .001$ *vs* Control pre-treatment.
§ $p < .001$ *vs* Control post-treatment.
$^{||}$ $p < .001$ *vs* LDE-DTX baseline.
$^{\#}$ $p < .05$ *vs* Control baseline.
† $p < .05$ *vs* Control pre-treatment.

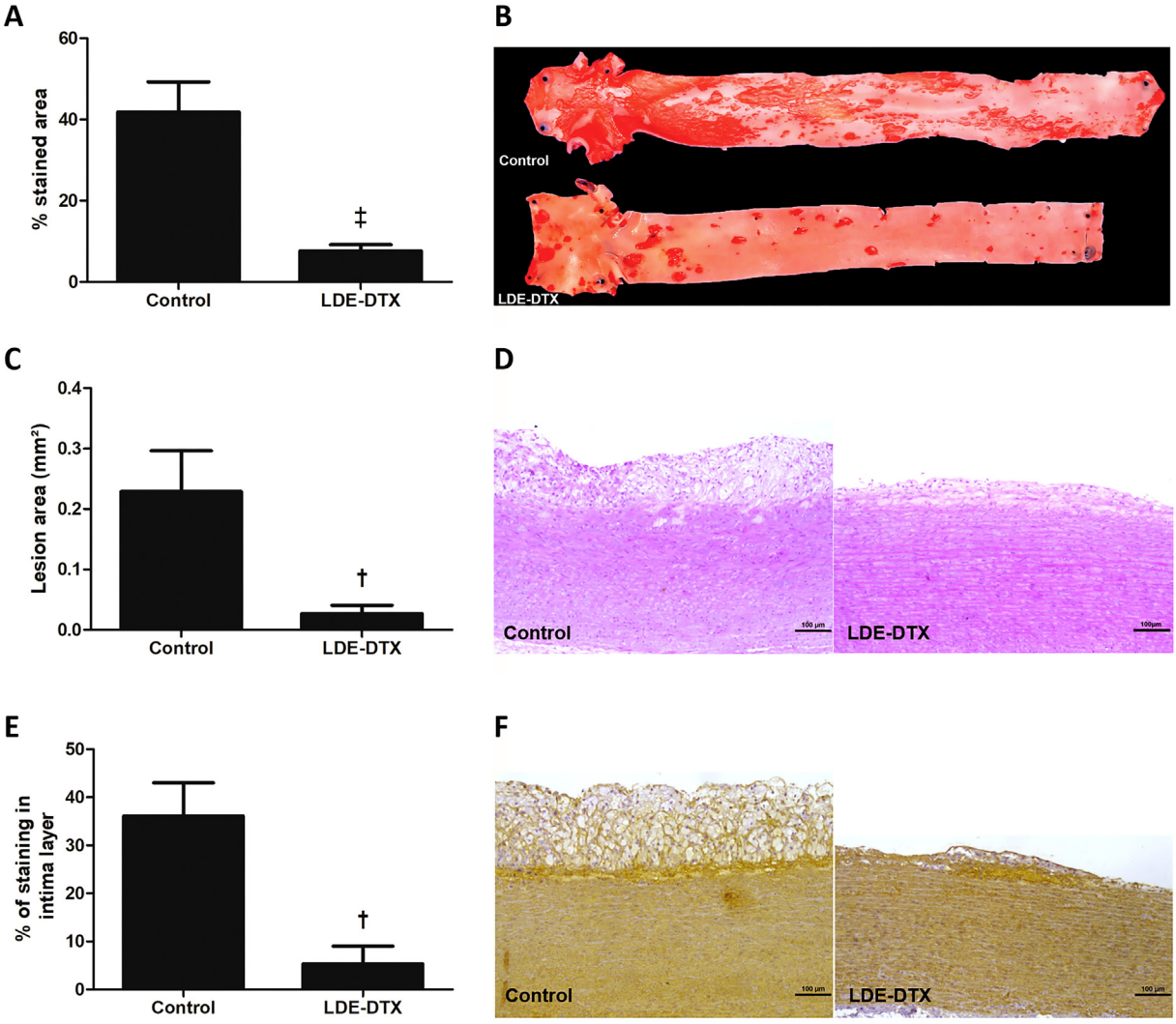

Fig. 2. Atherosclerotic plaques analysis: (A) Percentage of stained area of Control (n = 9) and LDE-DTX (n = 9) groups. $^{‡}p < .001$ *vs* Control group. (B) Representative images of aortas of Control and LDE-DTX groups with atherosclerotic lesions stained by Scarlat R (Sudan IV). (C) Percentage of microscopic lesion area of Control (n = 9) and LDE-DTX (n = 9) groups. $^{†}p < .01$ *vs* Control group. (D) Representative photomicrographs of aortic arch sections stained by hematoxylin-eosin of Control and LDE-DTX groups. Magnification: 100×. Bar represent 100 μm. (E) Percentage of immunostained area for VSMCs α-actin in intima layer of Control (n = 9) and LDE-DTX (n = 9) groups. $^{†}p < .01$ *vs* Control group. (F) Representative photomicrographs of aortic arch sections immunostained for VSMCs α-actin, identified in brown, of Control and LDE-DTX groups. Magnification: 100×. Bar represent 100 μm. Data are expressed as mean ± SEM in all plots. DTX, docetaxel. (For interpretation of the references to colour in this figure legend, the reader is referred to the web version of this article.)

2 and MMP-9 was about 70% lower in the LDE-DTX treated group compared to the Control group (Fig. 6B–C).

The protein expression of TGF-β was 50% lower in LDE-DTX treated animals than in Control group (Fig. 6D). Collagen 1 (Fig. 6E) was 30% lower in the LDE-DTX treated group, while collagen 3 (Fig. 6F) was about 70% lower in the LDE-DTX group when compared to the Control group. Fig. 6G shows a representative image of sections of aortic arch stained with Masson's trichrome depicting collagen in both Control and LDE-DTX groups.

4. Discussion

In this study, the treatment with the LDE-DTX preparation at 1 mg/kg/week dose resulted in about 80% decrease of atherosclerotic lesion area in the aorta of the cholesterol-fed rabbits. The reduction of the macrophage presence in the intima attained by LDE-DTX was 60%, whereas VSMCs presence was reduced by 85%. The cytotoxic action of the taxane was documented here in the aortic plaques: LDE-DTX inhibited by 40% the expression of PCNA, a scaffold protein involved in DNA replication that constitutes a standard proliferation marker.

Our previous study on the anti-atherosclerotic effects on rabbits of LDE-paclitaxel was the first in the literature to propose the systemic use of anti-cancer chemotherapeutic agents to treat cardiovascular diseases [6]. However, in that study, the effects of several parameters that are now being documented with LDE-DTX were not studied with LDE-paclitaxel, such as the action of taxanes associated to LDE on pro-inflammatory cytokines, apoptosis markers, metalloproteinases and vessel tissue structural and repair factors.

In fact, it is remarkable that the LDE-DTX action was favorable in all molecular aspects of anti-atherogenesis tested here. IL-1β, TNF-α and IL-6 protein expression, among the most well-established cytokines of pro-inflammatory, were inhibited. de la Llera-Moya et al. [20] had shown that treatment of cholesterol-fed rabbits with etoposide decreased the transformation of monocytes into macrophages thereby promoting atheroma regression. The decrease in macrophage presence in the intima by LDE-DTX can be accounted for the reduction of IL-1β, TNF-α and IL-6 expression, since macrophages are a major source of secretion of those cytokines.

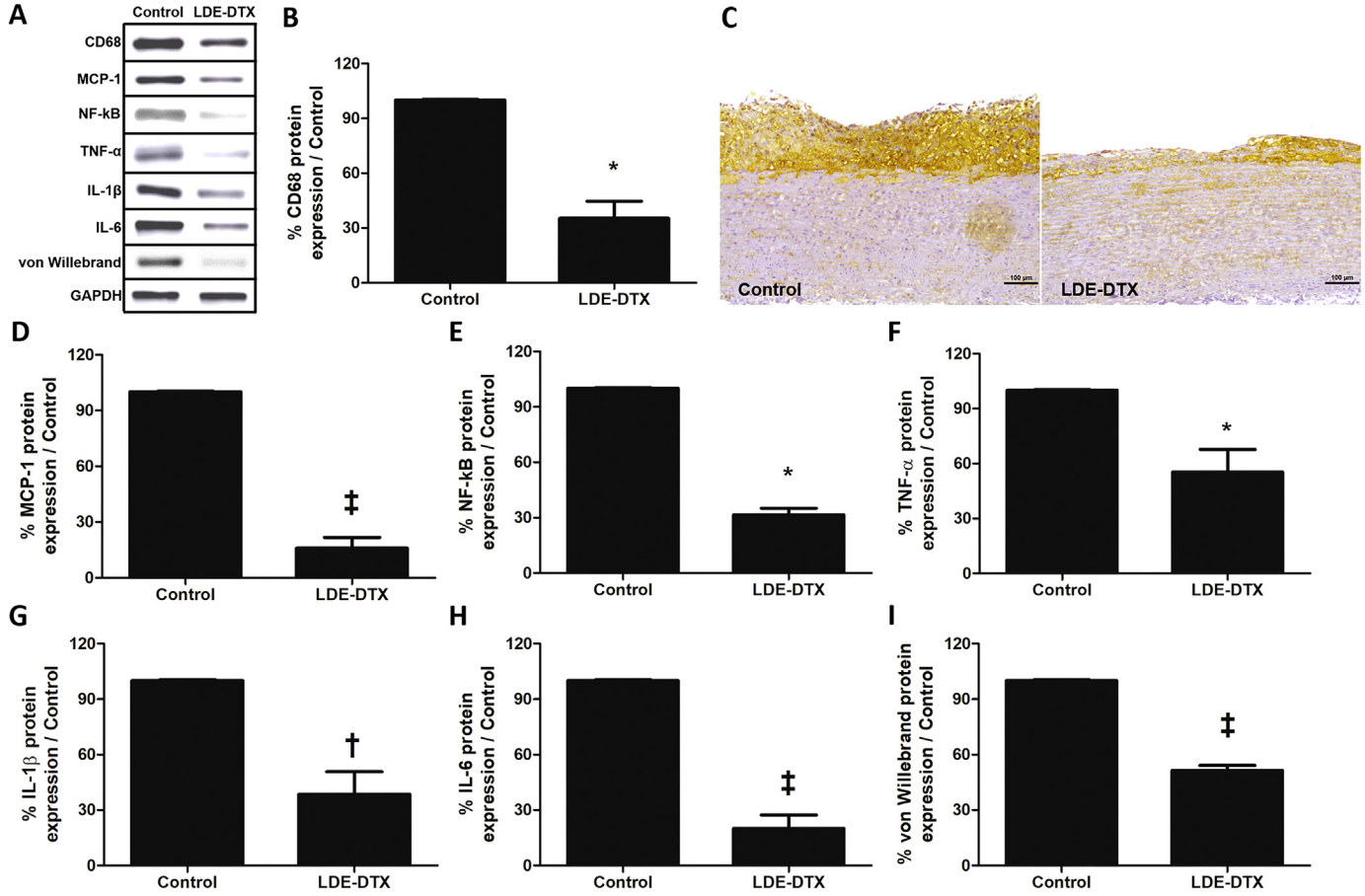

Fig. 3. Inflammation analysis. (A) Representative Western blot bands of inflammatory cells and inflammatory mediators of Control and LDE-DTX groups. (B) Western blot protein expression analysis of CD68 in aortic arch of Control (n = 4) and LDE-DTX (n = 5) groups. *p < .05 *vs* Control group. (C) Representative photomicrographs of aortic arch sections immunostained for macrophages, identified in brown, of Control and LDE-DTX groups. Magnification: 100×. Bar represent 100 μm. (D-I) Western blot protein expression analysis of the inflammatory mediators MCP-1 (D), NF-κB (E), TNF-α (F), IL-1β (G), IL-6 (H) and von Willebrand factor (I) in aortic arch of Control (n = 4) and LDE-DTX (n = 5) groups. *p < .05, ‡p < .001, and †p < .01 *vs* Control group. Data are expressed as mean ± SEM in all plots. DTX, docetaxel; CD68, cluster of differentiation 68; MCP-1, monocyte chemoattractant protein-1; NF-κB, nuclear factor kappa B; TNF-α, tumor necrosis factor α; IL, interleukin; GAPDH, glyceraldehyde 3-phosphate dehydrogenase. (For interpretation of the references to colour in this figure legend, the reader is referred to the web version of this article.)

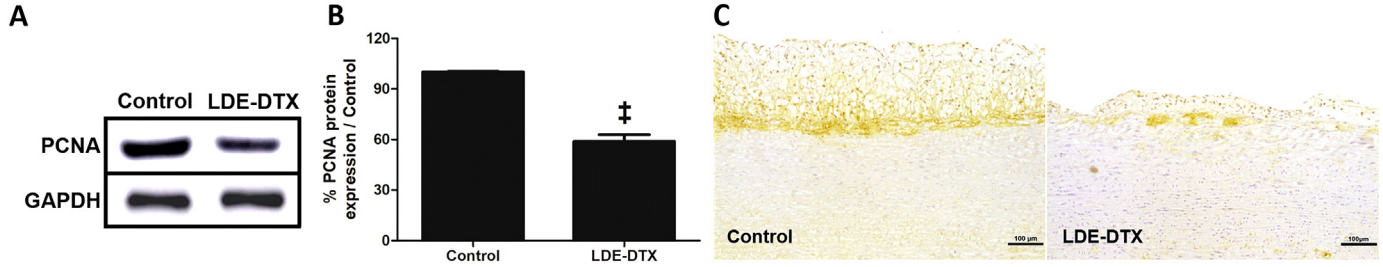

Fig. 4. Cell proliferation analysis. (A) Representative Western blot bands of PCNA proliferation marker of Control and LDE-DTX groups. (B) Western blot protein expression analysis of PCNA in aortic arch of Control (n = 4) and LDE-DTX (n = 5) groups. ‡p < .001 *vs* Control group. (C) Representative photomicrographs of aortic arch sections immunostained for PCNA, identified in brown, of Control and LDE-DTX groups. Magnification: 100×. Bar represent 100 μm. Data are expressed as mean ± SEM in all plots. DTX, docetaxel; PCNA, proliferating cell nuclear antigen; GAPDH, glyceraldehyde 3-phosphate dehydrogenase. (For interpretation of the references to colour in this figure legend, the reader is referred to the web version of this article.)

One of the observed actions of the LDE-DTX treatment was the reduction of the protein expression of MCP-1, a member of the C-C chemokine family that is produced by macrophages, endothelial cells and VSMCs [21]. The inhibition of MCP-1 might be involved in the marked reduction of macrophage presence in the intima of the LDE-DTX treated rabbits.

The anti-inflammatory action of LDE-DTX was also extended to vWF that is produced by the endothelium, since the protein expression in the aortic arch was decreased by the treatment. vWF has a presumptive role on leukocyte and platelet recruitment in inflamed tissue. It was recently implicated as another key mediator of vascular inflammation, and lines of evidence suggest its role in leukocyte and platelet recruitment in inflamed tissue. vWF can directly stimulate the proliferation of VSMCs, one of the major cell component of atheromas that was impaired by the LDE-DTX treatment [22].

A crucial finding in this study that may account for the above-

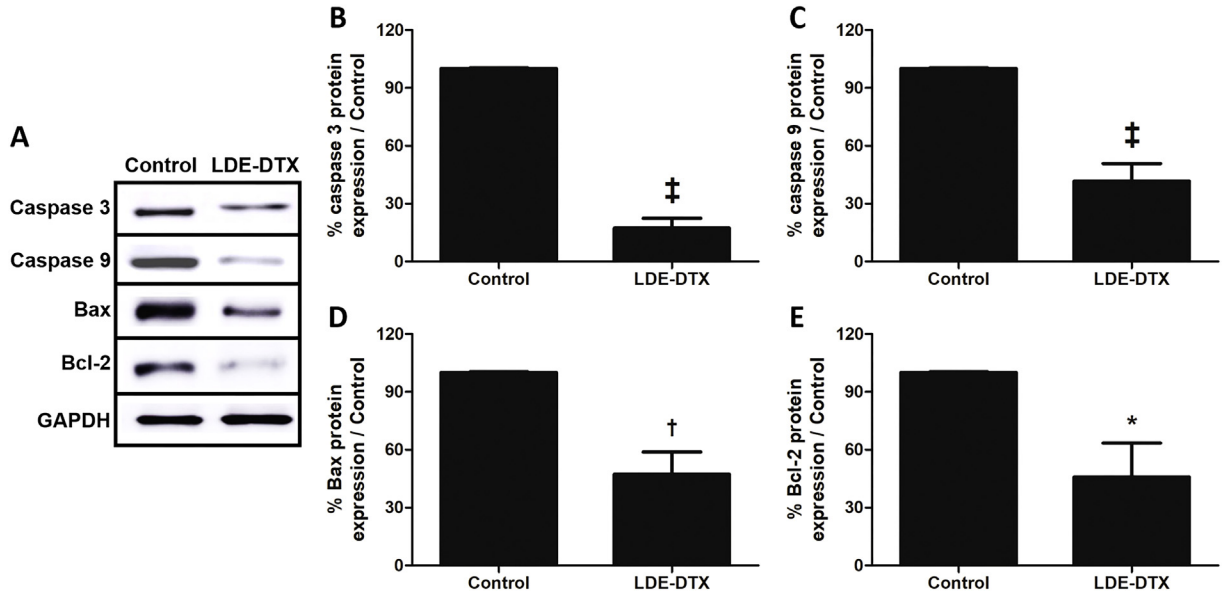

Fig. 5. Pro- and anti-apoptotic factors analysis. (A) Representative Western blot bands of pro- and anti-apoptotic factors of Control and LDE-DTX groups. (B-E) Western blot protein expression analysis of the pro-apoptotic factors caspase 3 (B), caspase 9 (C) and Bax (D), and of the anti-apoptotic factor Bcl-2 (E) in aortic arch of Control (n = 4) and LDE-DTX (n = 5) groups. ‡p < .001, †p < .01, and *p < .05 *vs* Control group. Data are expressed as mean ± SEM in all plots. DTX, docetaxel; Bax, bcl-2-like protein 4; Bcl-2, B-cell lymphoma 2; GAPDH, glyceraldehyde 3-phosphate dehydrogenase.

described results was the reduction of protein expression of NF-κB in the aortic arch by LDE-DTX treatment. NF-κB is a central mediator of the inflammatory process. In vascular endothelial cells, NF-κB mediates the induction of pro-inflammatory cytokines, chemotactic factors and adhesion molecules that promote the recruitment of monocytes and is also implicated in the conversion of macrophages to foam cells [23]. The pro-atherosclerotic feature of NF-κB stimuli has been documented in Apo-E knockout mice [24,25] and when inflammatory markers are lowered, the NF-κB expression is also reduced [26,27]. It is then possible that, at least in part, the effects of the LDE-DTX preparation on the several cytokines that resulted in anti-inflammatory action had been mediated through the inhibition of NF-κB.

The effects of LDE-DTX on the remodeling of the lesioned artery were approached here by estimating the protein expression of MMPs, collagen and TGF- β. MMPs secreted by macrophages degrade the extracellular matrix thereby facilitating the progression of cell migration and the invasion of the intimal layer by VSMCs from the media [28]. The amount and organization of matrix collagen is a major determinant of the mechanical stability of the fibrous cap and increase in the collagen proteolysis by MMPs is associated with plaque rupture. Increased MMPs are associated with thinner fibrous caps and less organized tissue structure [29]. TGF-β inhibits the accumulation of VSMCs in the intimal

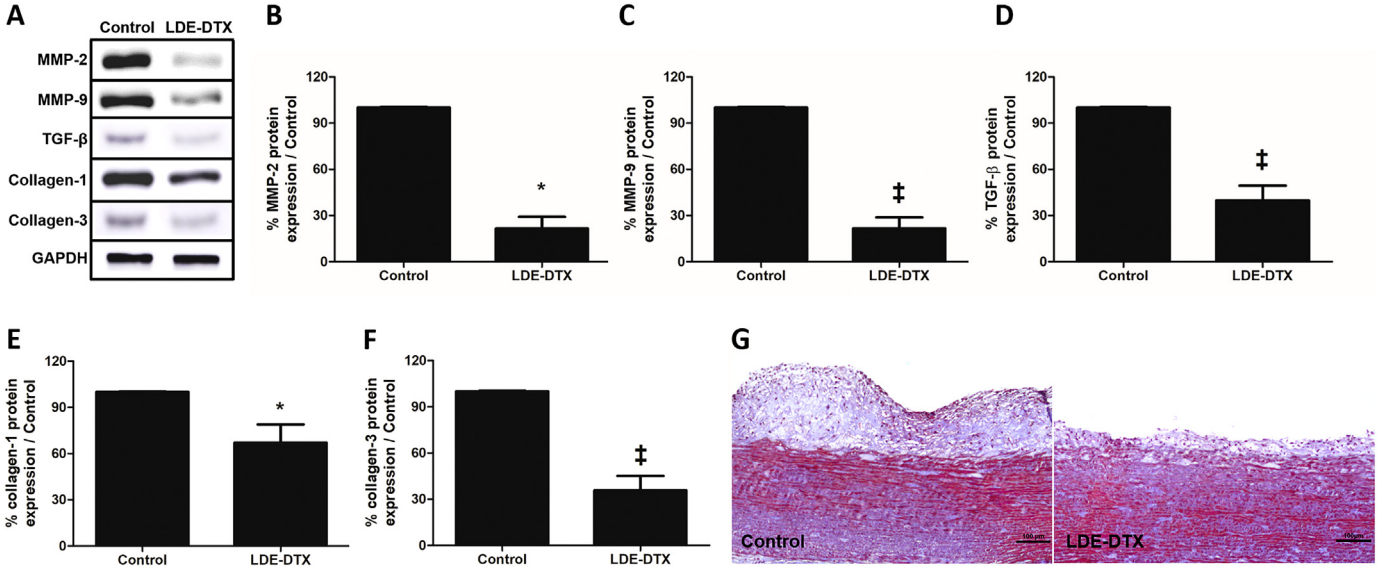

Fig. 6. Vascular repair analysis. (A) Representative Western blot bands of MMPs, TGF-β and collagens of Control and LDE-DTX groups. (B–F) Western blot protein expression analysis of MMP-2 (B), MMP-9 (C), TGF-β (D), collagen-1 (E) and collagen-3 (F) in aortic arch of Control (n = 4) and LDE-DTX (n = 5) groups. *p < .05, and ‡p < .001 *vs* Control group. Data are expressed as mean ± SEM in all plots. (G) Representative photomicrographs of aortic arch sections showing collagen, identified in blue, stained by Masson's trichrome of Control and LDE-DTX groups. Magnification: 100×. Bar represent 100 μm. DTX, docetaxel; MMP, metalloproteinase; TGF-β, transforming growth factor β; GAPDH, glyceraldehyde 3-phosphate dehydrogenase. (For interpretation of the references to colour in this figure legend, the reader is referred to the web version of this article.)

layer and stimulates the synthesis of extracellular matrix and the repair of the tissue of the arterial wall [30]. In the aortic arch of the atherosclerotic rabbits, treatment with LDE-DTX resulted in reduction of MMP-2, MMP-9, collagen I and collagen III, as well as of TGF-β. As the anti-blastic effect of DTX strongly inhibited the macrophage and VSMC invasion of the intima, it is conceivable that the reduction of the populations of those two cell types resulted in the diminished synthesis of MMPs and TGF-β by macrophages and of collagen by VSMCs.

It is interesting that the LDE-DTX treatment elicited reduction of either pro- or anti-apoptotic factors in the atherosclerotic aortic arch: pro-apoptotic caspases 3 and 9 and Bax, and anti-apoptotic Bcl-2 were all reduced in LDE-DTX group. The inflammatory cytokines present in the atherosclerotic lesion can lead to an enhanced apoptosis in the vessel wall and within the lesions. In fact, it is known that TNF-α stimulation of endothelial cells elicits pro-apoptotic signals, *via* dephosphorylation of Bcl-2 and activation of caspase 3 and in VSMCs the apoptosis signaling is through Fas ligand/Fas [31,32]. Atherosclerotic lesions with lower TNF-α expression showed reduced apoptotic cells and necrotic cores [33]. Thereby it would be expected, as we indeed found, that a lower expression of TNF-α in animals treated with LDE-DTX would reduce the pro-apoptoptic signaling and that this reduced stimuli would lead to a lower anti-apoptotic response.

The remarkable action of LDE in reducing of the drug toxicity was widely documented in studies with experimental animals and in patients with neoplastic and cardiovascular disease [6,10,13,15–18]. In this first study testing LDE-DTX, the lack of observable hematological, renal and hepatic toxicity by blood biochemistry was documented and should be further explored.

LDE-DTX showed strong capacity of reducing the atheroma lesion area and the macrophage and VSMCs invasion of the intima. The concerted actions of LDE-DTX on NF-κB and vWF, MCP-1, pro-inflammatory interleukins, cell proliferation and factors related with tissue repair such as MMPs and collagen expression, as well as cell apoptosis, all favored atherosclerosis regression. Our results suggest that this new formulation can be tested in future clinical trials aiming to achieve disease regression and strong and prompt prevention of the complications of atherosclerosis.

Conflict of interest

The authors declare that they have no conflict of interest.

Funding

This study was supported a grant from the State of São Paulo Research Support Foundation (FAPESP, São Paulo, Brazil), grant number 2014/03742-0.

Acknowledgments

Dr. Maranhão has a Research Career Award from the National Council for Scientific and Technological Development (CNPq, Brasília, Brazil).

References

[1] P. Libby, Inflammation in atherosclerosis, Nature 420 (2002) 868–874, https://doi.org/10.1038/nature01323.
[2] V.J. Dzau, R.C. Braun-Dullaeus, D.G. Sedding, Vascular proliferation and atherosclerosis: new perspectives and therapeutic strategies, Nat. Med. 8 (2002) 1249–1256, https://doi.org/10.1038/nm1102-1249.
[3] G.K. Hansson, P. Libby, The immune response in atherosclerosis: a double-edged sword, Nat. Rev. Immunol. 6 (2006) 508–519, https://doi.org/10.1038/nri1882.
[4] P.M. Ridker, B.M. Everett, T. Thuren, MacFadyen JG, W.H. Chang, C. Ballantyne, F. Fonseca, J. Nicolau, W. Koenig, S.D. Anker, Kastelein JJP, J.H. Cornel, P. Pais, D. Pella, J. Genest, R. Cifkova, A. Lorenzatti, T. Forster, Z. Kobalava, L. Vida-Simiti, M. Flather, H. Shimokawa, H. Ogawa, M. Dellborg, Rossi PRF, Troquay RPT, P. Libby, R.J. Glynn, CANTOS Trial Group, Antiinflammatory therapy with canakinumab for atherosclerotic disease, N. Engl. J. Med. 377 (2017) 1119–1131, https://doi.org/10.1056/NEJMoa1707914.
[5] A. Montero, F. Fossella, G. Hortobagyi, V. Valero, Docetaxel for treatment of solid tumours: a systematic review of clinical data, Lancet Oncol. 6 (2005) 229–239, https://doi.org/10.1016/S1470-2045(05)70094-2.
[6] R.C. Maranhão, E.R. Tavares, A.F. Padoveze, C.J. Valduga, D.G. Rodrigues, M.D. Pereira, Paclitaxel associated with cholesterol-rich nanoemulsions promotes atherosclerosis regression in the rabbit, Atherosclerosis (2008) 959–966, https://doi.org/10.1016/j.atherosclerosis.2007.12.051.
[7] D.D. Lourenço-Filho, R.C. Maranhão, C.A. Méndez-Contreras, E.R. Tavares, F.R. Freitas, N.A. Stolf, An artificial nanoemulsion carrying paclitaxel decreases the transplant heart vascular disease: a study in a rabbit graft model, J. Thorac. Cardiovasc. Surg. 141 (2011) 1522–1528, https://doi.org/10.1016/j.jtcvs.2010.08.032.
[8] R.C. Maranhão, M.C. Guido, A.D. de Lima, E.R. Tavares, A.F. Marques, M.D. Tavares de Melo, J.C. Nicolau, V.M. Salemi, R. Kalil-Filho, Methotrexate carried in lipid core nanoparticles reduces myocardial infarction size and improves cardiac function in rats, Int. J. Nanomedicine 17 (2017) 3767–3784, https://doi.org/10.2147/IJN.S129324.
[9] S.B. Mello, E.R. Tavares, M.C. Guido, E. Bonfá, R.C. Maranhão, Anti-inflammatory effects of intravenous methotrexate associated with lipid nanoemulsions on antigen-induced arthritis, Clinics 71 (2016) 54–58, https://doi.org/10.6061/clinics/2016(01)09.
[10] E.R. Tavares, F.R. Freitas, J. Diament, R.C. Maranhão, Reduction of atherosclerotic lesions in rabbits treated with etoposide associated with cholesterol-rich nanoemulsions, Int. J. Nanomedicine 6 (2011) 2297–2304, https://doi.org/10.2147/IJN.S24048.
[11] A. Bulgarelli, A.A. Martins Dias, B. Caramelli, R.C. Maranhão, Treatment with methotrexate inhibits atherogenesis in cholesterol-fed rabbits, J. Cardiovasc. Pharmacol. 59 (2012) 308–314, https://doi.org/10.1097/FJC.0b013e318241c385.
[12] E.M. Daminelli, A.E.M. Martinelli, A. Bulgarelli, F.R. Freitas, R.C. Maranhão, Reduction of atherosclerotic lesions by the chemotherapeutic agent carmustine associated to lipid nanoparticles, Cardiovasc. Drugs Ther. 30 (2016) 433–443, https://doi.org/10.1007/s10557-016-6675-0.
[13] F.L.T. Gomes, R.C. Maranhão, E.R. Tavares, P.O. Carvalho, M.L. Higuchi, F.R. Mattos, F.G. Pitta, S.A. Hatab, R. Kalil-Filho, C.V. Serrano Jr., Regression of atherosclerotic plaques of cholesterol-fed rabbits by combined chemotherapy with paclitaxel and methotrexate carried in lipid core nanoparticles, J. Cardiovasc. Pharmacol. Ther. 23 (2018) 561–569, https://doi.org/10.1177/1074248418778836.
[14] J. Vial, M. Cohen, P. Sassiat, D. Thiébaut, Pharmaceutical quality of Docetaxel generics versus originator drug product: a comparative analysis, Curr. Med. Res. Opin. 24 (2008) 2019–2033, https://doi.org/10.1185/03007990802207874.
[15] D.G. Rodrigues, D.A. Maria, D.C. Fernandes, C.J. Valduga, R.D. Couto, O.C. Ibañez, R.C. Maranhão, Improvement of paclitaxel therapeutic index by derivatization and association to a cholesterol-rich microemulsion: in vitro and in vivo studies, Cancer Chemother. Pharmacol. 55 (2005) 565–576, https://doi.org/10.1007/s00280-004-0930-y.
[16] L.A. Pires, R. Hegg, C.J. Valduga, S.R. Graziani, D.G. Rodrigues, R.C. Maranhão, Use of cholesterol-rich nanoparticles that bind to lipoprotein receptors as a vehicle to paclitaxel in the treatment of breast cancer: pharmacokinetics, tumor uptake and a pilot clinical study, Cancer Chemoter. Pharmacol. 2 (2009) 281–287, https://doi.org/10.1007/s00280-008-0738-2.
[17] S.R. Graziani, C.G. Vital, A.T. Morikawa, B.M. Van Eyll, H.J. Fernandes Junior, R. Kalil Filho, R.C. Maranhão, Phase II study of paclitaxel associated with lipid core nanoparticles (LDE) as third-line treatment of patients with epithelial ovarian carcinoma, Med. Oncol. 34 (2017) 151, https://doi.org/10.1007/s12032-017-1009-z.
[18] A.A. Shiozaki, T. Senra, A.T. Morikawa, D.F. Deus, A.T. Paladino-Filho, I.M. Pinto, R.C. Maranhão, Treatment of patients with aortic atherosclerotic disease with paclitaxel-associated lipid nanoparticles, Clinics 71 (2016) 435–439, https://doi.org/10.6061/clinics/2016(08)05.
[19] B. Meneghini, E. Tavares, M. Guido, T. Tavoni, H. Stefani, R. Kalil-Filho, R. Maranhão, Atherosclerotic plaques in aortas of rabbits treated with a lipid core nanoparticle (LDE) associated with docetaxel, Figshare. Figure (2018), https://doi.org/10.6084/m9.figshare.7429406.v1.
[20] M. de la Llera-Moya, G.H. Rothblat, J.M. Glick, J.M. England, Etoposide treatment suppresses atherosclerotic plaque development in cholesterol-fed rabbits, Arterioscler. Thromb. 12 (1992) 1363–1370.
[21] C. Gonzalez-Quesada, N.G. Frangogiannis, Monocyte chemoattractant protein (MCP-1)/CCL2 as a biomarker in acute coronary syndromes, Curr. Atheroscler. Rep. 11 (2009) 131–138.
[22] F. Gragnano, S. Sperlongano, E. Golia, F. Natale, R. Bianchi, M. Crisci, F. Fimiani, I. Pariggiano, V. Diana, A. Carbone, A. Cesaro, C. Concilio, G. Limongelli, M. Russo, P. Calabrò, The role of von Willebrand factor in vascular inflammation: from pathogenesis to targeted therapy, Mediat. Inflamm. 2017 (2017) 5620314, , https://doi.org/10.1155/2017/5620314.
[23] T. Liu, L. Zhang, D. Joo, S.C. Sun, NF-κB signaling in inflammation, Signal Transduct. Target Ther. 2 (2017) 17023, , https://doi.org/10.1038/sigtrans.2017.23.
[24] Bhat OM, Kumar PU, Harishankar N, Ravichandaran L, A. Bhatia A, Dhawan V (2017) Interleukin-18-induced cell adhesion molecule expression is associated with feedback regulation by PPAR-γ and NF-κB in Apo E−/− mice. Mol. Cell. Biochem. 428:119–128.
[25] R. Yao, X. Cheng, Y.H. Liao, Y. Chen, J.J. Xie, X. Yu, Y.J. Ding, T.T. Tang, Molecular mechanisms of felodipine suppressing atherosclerosis in high-cholesterol-diet

apolipoprotein E-knockout mice, J. Cardiovasc. Pharmacol. 51 (2008) 188–195, https://doi.org/10.1097/FJC.0b013e31815f2bce.
[26] J. Li, W. Wang, L. Han, M. Feng, H. Lu, L. Yang, X. Hu, S. Shi, S. Jiang, Q. Wang, L. Ye, Human apolipoprotein A-I exerts a prophylactic effect on high-fat diet-induced atherosclerosis via inflammation inhibition in a rabbit model, Acta Biochim. Biophys. Sin. 49 (2017) 149–158, https://doi.org/10.1093/abbs/gmw128.
[27] K.Y. Wang, A. Tanimoto, X. Guo, S. Yamada, S. Shimajiri, Y. Murata, Y. Ding, M. Tsutsui, S. Kato, T. Watanabe, H. Ohtsu, K. Hirano, K. Kohno, Y. Sasaguri, Histamine deficiency decreases atherosclerosis and inflammatory response in apolipoprotein E knockout mice independently of serum cholesterol level, Arterioscler. Thromb. Vasc. Biol. 4 (2011) 800–807, https://doi.org/10.1161/ATVBAHA.110.215228.
[28] S.K. Nadkarni, B.E. Bouma, J. de Boer, G.J. Tearney, Evaluation of collagen in-atherosclerotic plaques: the use of two coherent laser-based imaging methods, Lasers Med. Sci. 24 (2009) 439–445, https://doi.org/10.1007/s10103-007-0535-x.
[29] N. Hakimzadeh, V.A. Pinas, G. Molenaar, V. de Waard, E. Lutgens, B.L.F. van Eck-Smit, K. de Bruin, J.J. Piek, J.L.H. Eersels, J. Booij, H.J. Verberne, A.D. Windhorst, Novel molecular imaging ligands targeting matrix metalloproteinases 2 and 9 for imaging of unstable atherosclerotic plaques, PLoS One 12 (2017) e0187767, , https://doi.org/10.1371/journal.pone.0187767.
[30] I. Toma, T.A. McCaffrey, Transforming growth factor-β and atherosclerosis: interwoven atherogenic and atheroprotective aspects, Cell Tissue Res. 347 (2012) 155–175, https://doi.org/10.1007/s00441-011-1189-3.
[31] S. Dimmeler, K. Breitschopf, J. Haendeler, A.M. Zeiher, Dephosphorylation targets Bcl-2 for ubiquitin-dependent degradation: a link between the apoptosome and the proteasome pathway, J. Exp. Med. 189 (1999) 1815–1822, https://doi.org/10.1084/jem.189.11.18150.
[32] J.J. Boyle, P.L. Weissberg, M.R. Bennett, Tumor necrosis factor-alpha promotes macrophage-induced vascular smooth muscle cell apoptosis by direct and autocrine mechanisms, Arterioscler. Thromb. Vasc. Biol. 23 (2003) 1553–1558, https://doi.org/10.1161/01.ATV.0000086961.44581.B7.
[33] C. Tay, Y.H. Liu, H. Hosseini, P. Kanellakis, A. Cao, K. Peter, P. Tipping, A. Bobik, B.H. Toh, T. Kyaw, B-cell-specific depletion of tumor necrosis factor alpha inhibits atherosclerosis development and plaque vulnerability to rupture by reducing cell death and inflammation, Cardiovasc. Res. 111 (2016) 385–397, https://doi.org/10.1093/cvr/cvw186.